

## CHARACTERIZATION OF WAKE DYNAMICS VIA PROPER ORTHOGONAL DECOMPOSITION FOR VARYING WIND FARM ARRANGEMENTS

Nicholas Hamilton<sup>1</sup>, Murat Tutkun<sup>2</sup> & Raúl Bayoán Cal<sup>1</sup>

<sup>1</sup>*Department of Mechanical and Materials Engineering, Portland State University, Portland, OR, USA*

<sup>2</sup>*The Norwegian Defense Research Establishment, Kjeller, Norway*

**Abstract** Comparison of the dynamics between a standard rectilinear array and two offset row configurations. Stereo particle-image-velocimetry is used to collect a large sample of data ahead of and behind entrance and exit row turbines in each configuration. Inflow and wakes are compared statistically and through proper orthogonal decomposition (POD). Spacing within the array configurations lead to varied wake recovery conditions visible in statistics and POD analysis. The number of snapshot POD modes required to reconstruct specified energy levels for the wakes demonstrates a strong dependence on the array configuration. Quantities including flux of kinetic energy and production rebuild with fewer POD modes than vorticity and dissipation as they rely on large-scale structures for shape and intensity. Energy content and organization in small-scale structures contribute to the delay of recovery of the flow to upstream inflow conditions.

### EXPERIMENTS & RESULTS

Experiments are carried out in the Portland State University wind tunnel. The rectangular arrangement (referred to from here as the base case) was set such that each subsequent wind turbine models were directly downstream of the preceding rows. This geometry is typical in real installations for both on- and offshore conditions. The geometrical change to the array seed in the row-offset configuration consisted of a spanwise shift of 1.5 rotor diameters for alternating rows. With this modification, wind turbine wakes were given twice the streamwise distance to recover toward the unloaded atmospheric boundary layer (ABL) without significantly altering the density of wind turbines per unit area of land. The turbines themselves consisted of several key components. Wind turbine rotors were manufactured in house from a thin sheet of steel. Each blade in the rotor was given a 15° pitch at the root of the blade and a 5° twist from root to tip with a die press to ensure consistency. The nacelles of each wind turbine consisted of an electric motor with low friction bearings. When powered by the interaction of the rotor blades and the ABL, the electric motors act as generators and produce measureable signals. Loading electrical circuits containing the electrical generators enabled specific and sensitive control of the angular frequency of the rotors. Stereo particle image velocimetry (SPIV) was used to collect data directly upstream and downstream of wind turbine models simultaneously in entrance and exit rows of each wind turbine array configuration. The flux of kinetic energy quantifies the vertical entrainment of kinetic energy from above the turbine canopy into the wake areas following an obstruction. This quantity has been linked to the rate of recovery of wakes and was shown to persist into the very far-wake region ( $x/D > 10$ ). Comparing the base case to the row-offset case showed that the flux of kinetic energy was increased by approximately 15% in the maximum for the exit row of the row-offset case. The flux of kinetic energy also demonstrated much more concentrated regions of high intensity in the row-offset case compared to the basic case. The increased concentration is a product of a more recovered ABL as inflow to exit row turbines.

Trends in power followed expectations well in that entrance row turbines of both cases were very similar and were significantly greater than those of exit row turbines. Also agreeing well with intuition was that the exit row turbine of the base case performed less well than that of the offset case. An exit row turbine of the base case has three turbines directly upstream of it each spaced at only 6 rotor diameters. Thus the inflow to that particular turbine is reduced as is the power produced. In the offset case, there is only one turbine upstream of the exit row and it is also given twice the streamwise spacing. The exit row turbine in the offset case produced approximately 3.5 times the power of the base case and approximately 60% of the power seen in entrance row turbines in either case. This is further stated by looking at the summation of eigenvalues upstream and downstream of the turbines, which essentially represents the energy extracted out of the turbine. Small magnitudes of  $\mathcal{E}$  correspond to greater power production. This agrees with intuition in that  $\mathcal{E}$  relates the turbulence energy upstream and downstream of the wind turbines. Therefore, it is found that for the inflow of canopy the greatest energy is extracted as expected with  $\mathcal{E} = 0.21$ , then follows the staggered case within the canopy ( $\mathcal{E}=0.29$ ) and finally the turbine in the aligned case within the canopy ( $\mathcal{E}=0.34$ ).

$$\mathcal{E} = \frac{E_{upstream}}{E_{downstream}} = \frac{\sum_{n=1}^{2000} \lambda_{upstream}}{\sum_{n=1}^{2000} \lambda_{downstream}} \quad (1)$$

Additional analysis was performed on the SPIV data in the form of the Proper Orthogonal Decomposition (POD). The method of snapshots (snapshot POD) was used in this case to maintain the high spatial resolution of SPIV images and account for the low temporal resolution of the system. Snapshot POD consists of formulating a set of orthogonal functions

(POD modes) that and associated coefficients from the kernel basis of the correlation tensor from the SPIV data. The eigenvalues associated with each POD mode are representative of the turbulent kinetic energy contained in the structures organized in that mode. The benchmark used in comparing the rate of energy reconstruction of the various measurement locations was the number of modes required to reconstruct fields with 50% of the total energy as defined by a cumulative summation of the ordered eigenvalues. It was shown that the rate of reconstruction of the energy was highly dependent on the distribution of energy in the turbulence. Thus when the energy in the turbulence is distributed evenly throughout a large range of scales, the reconstruction of 50% energy requires more modes than if the energy is concentrated in only the larger structures. These decompositions are noted in figure 1. The different cases will be explained in the full paper.

In this analysis it was shown that the energy reconstructed most quickly in the wake area of the exit row turbine of the offset case. This indicates that there is a greater concentration of energy in the large structures at that location compared to the other wake areas. The exit row of the base case required 4 times as many POD modes to reconstruct 50% of the total turbulent kinetic energy for that location. This result implies that the turbulent energy is distributed over a greater range of scales in the exit row of the base case than in the offset case. This is also visually observed where in figure 2, it is shown the exit planes for the first row turbine (left), last row turbine in aligned case (middle) and last row turbine in staggered case (right). This is demonstrative that the vertical entrainment of kinetic energy is reliant on only the large structures of turbulence and the relative shape and magnitudes between the left and right contour plot allow for greater energy extraction as also shown by the power as well as equation 1. Because turbulence is a three dimensional phenomenon and it tends to greatly increasing mixing rates and transport, an *increase* of turbulence kinetic energy in the near wake can lead to a shorter recovery length of the wake. The increased energy of large structures in the upper wake area tends to increase the energy entrained from above into the turbine canopy. Other arrangements will be sought as part of the paper.

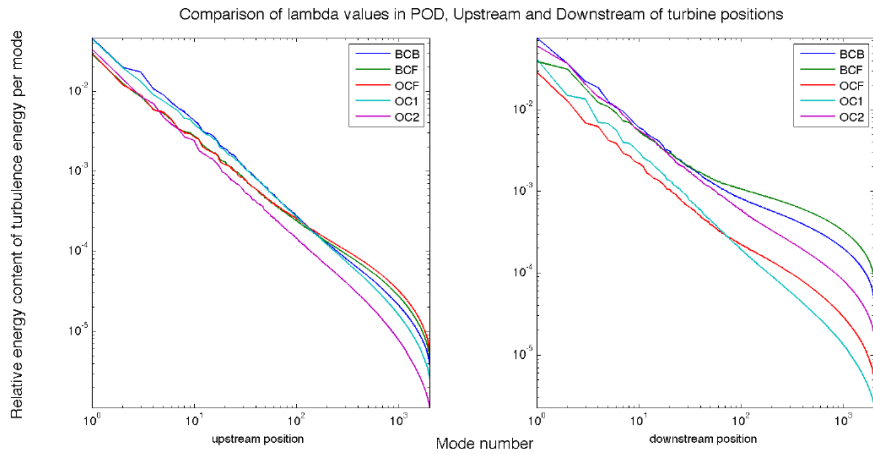


**Figure 1.** Comparison of values for each measurement position. The subplot on the left is the upstream location for each case and the right is downstream. Note that the first mode for all cases is higher downstream than upstream. Here, all eigenvalues were normalized by the maximum sum, the sum of eigenvalues corresponding to the downstream window of BCF.

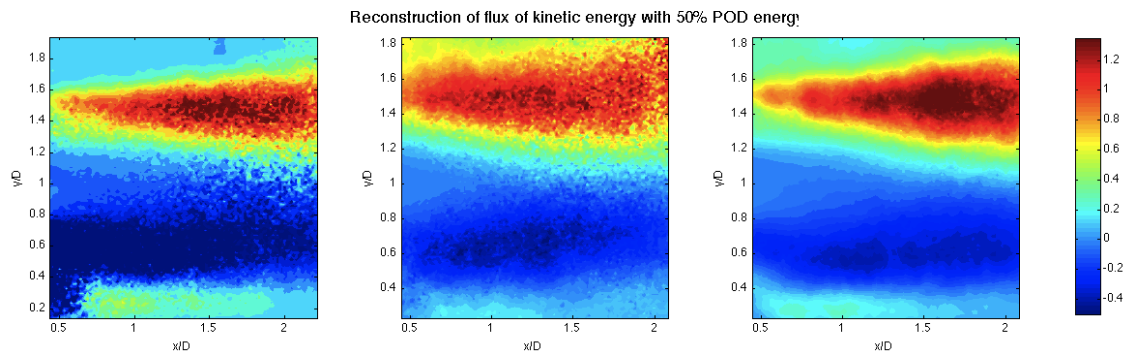


**Figure 2.** Reconstructions of the flux of kinetic energy  $F_{ij}$  for the immediate wake areas. From left to right, first row turbine, last row turbine in aligned case and last row turbine in staggered case.